Send Orders for Reprints to reprints@benthamscience.net

Current Drug Delivery, 2023, *20*, 830-840

RESEARCH ARTICLE

Ketorolac Tromethamine Loaded Nano-Spray Dried Nanoparticles: Preparation, Characterization, Cell Viability, COL1A1 Gene Simulation and Determination of Anti-inflammatory Activity by *In vivo* HET-CAM Assay



A.A. Öztürk[1,*], T. Çevikelli[2], E.K. Tilki[3], U.M. Güven[2] and H.T. Kıyan[4]

[1]*Department of Pharmaceutical Technology, Faculty of Pharmacy, Anadolu University, Eskişehir, Türkiye;* [2]*Department of Pharmaceutical Technology, Faculty of Pharmacy, Çukurova University, Adana, Türkiye;* [3]*Department of Pharmacology, Faculty of Pharmacy, Anadolu University, Eskişehir, Türkiye;* [4]*Department of Pharmacognosy, Faculty of Pharmacy, Anadolu University, Eskişehir, Türkiye*

© 2023 The Author(s). Published by Bentham Science Publisher. This is an open access article published under CC BY 4.0 https://creativecommons.org/licenses/by/4.0/legalcode

ARTICLE HISTORY

Received: September 28, 2022
Revised: November 09, 2022
Accepted: December 12, 2022

DOI:
10.2174/1567201820666230125144133

Abstract: ***Background:*** Ketorolac tromethamine (KT) is a non-steroidal anti-inflammatory drug from the heteroaryl acetic acid derivatives family. The most widely used new nanotechnological approaches for topical drug delivery are polymeric nanoparticles (NPs).

Objective: Successful results have been obtained with low doses in many treatments, such as cancer, antimicrobial, pain, made with nanoparticle formulations of drug active ingredients.

Methods: NPs were prepared using Nano Spray-Dryer. The cytotoxicity of the optimum formulation in BJ (ATCC® CRL-2522™) human fibroblast cells was determined by the WST- 1 method and the gene activity was elucidated by mRNA isolation and real-time polymerase chain reaction (RT-PCR). The *in vivo* HET- CAM assay was performed for anti-inflammatory activity.

Results: NPs presented PDI values lower than 0.5, and therefore particle size distribution was decided to be monodisperse. Positive zeta potential values of NPs highlighted the presence of the cationic ammonium group of Eudragit® RS 100. The release rates observed from KT-NP coded formulations after 24 hours were 78.4% ± 2.9, demonstrating extended release from all formulations, relative to pure KT. The lowest concentration of KT-NP increased fibroblast cell proliferation higher than the highest concentration of KT. The 5-fold increased effect of KT-NP formulation on collagen gene expression compared to KT is also related to the enhanced anti-inflammatory effect in line with the *in vivo* HET-CAM assay results.

Conclusion: With the obtained cell viability, gene expression, and HET-CAM results, it has the hope of a successful nano-topical formulation, especially in both wound healing and anti-inflammatory treatment.

Keywords: Ketorolac tromethamine, wound, HET-CAM, RT-PCR, COL1A1, nanoparticle, KT-NP.

1. INTRODUCTION

The process of creating a novel therapeutic molecule is not only time-consuming and expensive, but it also frequently fails. However, a more efficient way to employ these medications in the clinic may be to increase their bioavailability, targeting, efficacy, or safety using a variety of techniques. The researchers have explored a variety of approaches in-depth, including targeted medication therapy that is stimulant-sensitive, drug conjugates, therapeutic drug monitoring, and nanoparticle (NP)-based drug delivery systems [1, 2]. High-dose treatments with traditional drugs can be performed at lower doses with systems such as NPs, and high effects can be obtained at low doses [3-5]. NP-based therapies have a wide range of applications nowadays, and advances in nanotechnology offer novel solutions to disease problems. Recently, nanodelivery systems are rapidly developing new materials in the nanoscale range that are employed to deliver therapeutic agents to specific targeted sites in a controlled manner. It has presented a variety of fascinating healthcare prospects, and a few items are currently on the market [6]. In many cases, such as cancer [7-9], conditions caused by microorganisms [10], pain [11], oxidative induced diseases [12, 13], and COVID-19 [14], the gaps in the treatment with nanoparticle systems are tried to be filled, and treatment with nanoparticles is a path to success.

NPs made with natural polymers, polymeric NPs, nanoemulsions, lipid-based nanoparticles, metal nanoparticles,

*Address correspondence to this author at the Department of Pharmaceutical Technology, Faculty of Pharmacy, Anadolu University, P.O. Box: 26470, Eskişehir, Türkiye; Tel/Fax: +90 222 335 05 80 /3731; E-mail: aaozturk@anadolu.edu.tr

Current Drug Delivery

and dendrimers are the most often employed innovative nanotechnological techniques for topical drug delivery [15]. An essential technology that is quick, easy, repeatable, and scalable is spray drying. It can be used in a variety of settings, including food, chemicals, and the encapsulation of medications. The two types of spray drying in technology are traditional and nano. The creation of drug-loaded nanosized particles for use in a variety of drug delivery applications is the primary benefit of nano spray drying. The manufacturing of submicron spray-dried particles was made possible by recent advancements in nano spray drier technology and the 2009 market introduction of the Nano Spray Dryer B-90 by Büchi Labortechnik AG [16]. Therefore, one of the pharmaceutical industry processes that has been the most thoroughly investigated is spray drying. Drug formulations for topical application are commonly employed. A copolymer of ethyl acrylate, methyl methacrylate, and methacrylic acid ester containing quaternary ammonium groups is called Eudragit RS 100 (ERS). The polymers are permeable because of the ammonium groups, which are present as salts [17].

A non-steroidal anti-inflammatory drug from the heteroaryl acetic acid derivatives family, ketorolac tromethamine (KT) is used to treat inflammation. It is a non-selective racemate type of cyclooxygenase (COX) inhibitor. Most of the analgesic and COX inhibitory effects of the S-isomer are still present. Ketorolac is administered as its tromethamine salt orally, intramuscularly, intravenously, and as a topical ophthalmic solution. Numerous formulation strategies for the suitable distribution of KT have been devised due to the frequent occurrence of gastrointestinal problems like gastrointestinal bleeding, perforation, and peptic ulcers as well as the short mean plasma half-life ($t_{1/2} \cong 5.5$ h) [18]. KT is frequently used successfully for surgical wounds and post-surgical (postoperative) pain [19].

Anti-inflammation is a favorable reaction to a treatment that reduces inflammation, which has an impact on the central nervous system. Wound healing is a process of tissue regeneration that includes inflammation as an early step. There are three stages of wound healing: acute, proliferative, and remodeling wounds. The wound may heal more slowly because of drug therapy, which can occasionally slow these wound healing processes. Novel anti-inflammatory medications may therefore be created that do not interfere with these systems [20].

The chronic nature of nonhealing wounds, as well as the difficulties that come with them, has prompted the development of nanotechnology-based therapies aimed at speeding up the healing process and, ultimately, mending the damaged tissue. A number of designed nanotechnologies with unique features and numerous roles have been proposed to solve specific issues with wound repair mechanisms [21]. Fibre-forming collagen type I, encoded by the COL1A1 gene, is the most common collagen in the skin, accounting for 90% of the total. The systemic organization of tissue is crucial for wound healing as it is vital to its integrity and strength. If the physiologically inflammatory response in wound healing is prolonged or exacerbated, it leads to a delay in the later stages of proper wound healing. In this case, anti-inflammatory agents are needed [22].

The *in vivo* Hen's Egg Test on the Chorioallantoic Membrane (HET-CAM) assay is extremely beneficial, affordable, and easy to use. It is sensitive to both steroidal and non-steroidal agents and is well established for screening the potency of natural products like plant extracts and essential oils, as well as synthetic therapeutics, drug formulations, and cosmetics, for their ability to reduce inflammation, prevent teratogenicity, and possibly cause toxic and adverse side effects [23-25].

Within the scope of this study, KT loaded nanoparticle-based drug delivery systems, which can be effective in pain treatment and wound healing processes in postoperative conditions, were prepared. After the characterization procedures, the cytotoxicity of the optimum formulation in human fibroblast cells was determined by the WST- 1 method and the gene activity was elucidated by mRNA isolation and real-time polymerase chain reaction (RT-PCR). The *in vivo* HET-CAM assay was performed on the selected optimum formulation for anti-inflammatory activity.

2. MATERIALS AND METHODS

2.1. Materials

KT is kind gift from Deva İlaç (Istanbul, Turkey). ERS is a kind gift from Evonik Nutrition & Care GmbH (Darmstadt, Germany). The fertilized eggs used in the HET-CAM test were obtained from Has Tavuk Company (Bursa and Sivrihisar, Turkey). All other chemicals used were of analytical grade.

2.2. Preparation of Nanoparticles

NPs were prepared using Nano Spray-Dryer (B-90, Büchi Labortechnik AG, Switzerland) [17, 24]. For the preparation of NPs, ERS was dissolved in methanol prior to the addition of KT. Spray-drying conditions and NPs ingredients are summarized in Tables **1** and **2**, respectively.

2.3. Particle Size, Polydispersity Index and Zeta Potential

Particle size (PS), polydispersity index (PDI) and zeta potential (ZP) of NPs were analyzed by a Zetasizer Nano ZS (Malvern Instruments, UK) [26-28]. Morphological and structural characteristics of the NPs prepared were investigated using SEM (FEI Quanta FEG 650, US).

2.4. Encapsulation Efficiency and Dissolution

UPLC device (Agilent Technology 1290 Infinity) used was mounted with reversed-phase (RP) Zorbax Eclipse Plus C_{18} gravity column (column length: 50 mm, column diameter: 2.1 mm, particle diameter: 1.8 μm). 50:50 (v/v) Water: Acetonitrile was used as the mobile phase for perfect resolution of KT. Flow rate of the mobile phase was set at 0.25 $mL.min^{-1}$, and 0.5 μL invariable volume of the specimen was injected by an automatic injector. The temperature of the column was set to 40°C while a fluorescent detector was used at 315 nm [29, 30].

Accurately weighed NPs (2 mg) were dispersed in distilled water (10 mL), vortexed for 1 min and centrifuged at 13.000 rpm for 15 min for the determination of KT left on NPs' surface (KT_s). After centrifugation, the supernatants were collected, and all solutions were filtered through a

Table 1. Spray-drying conditions.

Inlet Temperature	Outlet Temperature	Pump Level	Spray Level
100°C	54°C	4	100%

Table 2. NPs ingredients.

Code	ERS	KT	Methanol
KT-Blank (KT-B / KT-B-NP)	1 g	-	100 mL
KT-NP	1 g	0.4 g	100 mL

0.22 µm polyamide filter and analyzed using UPLC. The quantity of KT entrapped in NPs was calculated as the difference between the initially added (KT_t) and the KTs. Each experiment was repeated three times for statistical analysis and the average values and standard deviation (Mean ± SD) of the measurements were calculated. Entrapment efficiency was expressed as EE (%) and calculated with Eq. (**1**) [28, 27].

$$EE\ \% = \left[\frac{KT_t - KT_s}{KT_t}\right] x\ 100 \quad (1)$$

The *in vitro* dissolution studies of KT-loaded NP were performed using the dialysis bag diffusion technique equipped with a magnetic stirrer (IKA® Labor Technik RT 15 S000, Germany) at a speed of 100 rpm. Briefly, 10 mg of KT and NPs containing KT equivalent to 10 mg KT was suspended in 1 mL of pH 6.8 buffer and transferred into a dialysis bag (Dialysis tubing cellulose membrane average flat width 33 mm (1.3 in.), Mw cut-off (MWCO): 14.000, D9652, Sigma-Aldrich, USA). The dialysis bags were placed into a beaker containing 100 mL of pH 6.8 buffer at 37 ± 1°C. The receptor compartment/beaker was closed to prevent evaporation of the release medium. Samples of the medium (2 mL) were withdrawn and replaced with fresh medium at 1, 2, 3, 4, 5, 6, 9, 12 and 24 hours. KT concentration in the samples was quantified by UPLC. The *in vitro* dissolution study was repeated three times for KT-NP and pure KT, then the results were calculated as Mean ± SD. The results were then plotted as the cumulative release.

2.5. *In vitro* Pharmacological Characterizations

2.5.1. Cell Culture

BJ (American Type Culture Collection (ATCC®) CRL-2522™) human fibroblast cells were cultured in 10% fetal bovine serum and 1% penicillin/streptomycin containing Eagle's Minimum Essential Medium (EMEM) growth medium at 37°C in a humidified incubator with 5% CO_2. Cells were passaged when the proliferated cells reached 70-80% density at the bottom of the flask and transferred to new flasks or cell stocks were prepared for the next experiments. Prior to the experiments, cells were stained with Trypan blue solution and the cell counter Cedex XS (Roche-Innovatis, Germany) were used to determine the appropriate cell numbers.

2.5.2. Cell Viability Assay

Cell viability of BJ cells was measured using a colorimetric assay for 96- well plates with WST-1 (2-(4-iodophenyl)-3-(4-nitrophenyl)-5-(2, 4-disulfophenyl)-2 H-tetrazolium monosodium salt) reagent. In principle, WST-1 works by reacting with the mitochondrial succinate-tetrazolium reductase forming the formazan dye. This reagent produces a water-soluble formazan; therefore, the WST-1 reaction product can be quantified in 0.5 to 4 h without an additional solubilization step [31].

To evaluate the effects of the samples, BJ cells were seeded in 96-well plates at a density of 5×10^3 cells per well. After 24 hours, controls, KT, KT-Blank and KT-NP were added to wells at 25, 50, 100, 200 and 400 $\mu g.mL^{-1}$ concentrations and incubated for another 24 hours. At the end of the incubation, 10 µl WST-1 solution was added to each well and after 3 hours, the absorbances were measured at 450 nm using a Cytation 3 Cell Imaging Multi-Mode Reader (BioTek, USA) according to the WST-1 kit protocol (Catalog no: 11644807001, Roche, Germany). The measured absorbance directly correlates with the number of viable cells. Cell viability rates were expressed as a percentage of the control value [32, 33]

2.5.3. mRNA Isolation and Real-Time Polymerase Chain Reaction (RT-PCR)

To investigate the gene expression levels of collagen type 1 alpha 1 chain (COL1A1) gene related with wound healing, $1x10^6$ BJ cells were seeded at 6-well plates. After 24 hours, cells were treated with 25, 100 and 400 $\mu g.mL^{-1}$ KT and KT-NP concentrations and incubated for 24 hours. After the incubation period, mRNA was isolated from the cells. mRNA isolations were performed in MagNA Pure Compact System (Roche, Germany) using MagNA Pure Compact RNA Isolation Kit® (Catalog No: 04802993001, Roche, Germany). The total mRNA amounts of the samples were measured at 260 and 280 nm in the NanoDrop 2000® (Thermo Fisher, USA) spectrophotometer. cDNA was obtained using the Transcriptor High Fidelity cDNA Synthesis Kit® (Catalog no: 05091284001, Roche, Germany) following the kit protocol from 500 $ng.\mu l^{-1}$ mRNA of each sample. After the cDNA samples were replicated by PCR method, the expression levels were determined with the LightCycler® 480 Real-Time PCR System (Roche, Germany) using the COL1A1 primer (Real-Time Ready Assay, Assay ID: 100861, Roche, Germany). Glucose-6-phosphate dehydrogenase (G6PD) was used as a housekeeping gene. Primer IDs and RT-PCR cycling conditions are shown in Tables **3** and **4**. Results were analyzed according to the changes in the amplification levels

Table 3. Primer names and ID used for real-time PCR.

Gene	Gene ID	Accession ID
COL1A1	1277	ENST00000225964
G6PD	2539	ENST00000393562

Table 4. RT-PCR cycling conditions.

Step	Heat	Duration	Cycle
Incubation	95°C	10 min	1
Amplification	95°C 60°C 72°C	10 s 30 s 1 s	45
Cooling	40°C	30 s	1

Table 5. The semi quantitative score system of anti-inflammatory effect on CAM after treatment.

Category	Type	Effects Observed on CAM After Treatment
1	Irritated	The granuloma is strongly vascularized. A network of capillaries is formed star-like around the granuloma.
2	Weakly irritated	The granuloma is poorly vascularized. A thin network of capillaries is formed star-like around the granuloma.
3	Weakly normalized	The granuloma is somewhat smaller than in categories 1 and 2 and only poorly vascularized. The star-like network of vessels is hardly recognizable.
4	Normalized	No granuloma or only a kind of ‘‘scar’’ can be observed (if the granuloma regresses a non-vascularized scar is left). The network of vessels is normal (as the control).

compared to the control group with the analysis software of the instrument.

2.6. *In vivo* Anti-inflammatory Activity by Hen’s Egg Test on the Chorioallantoic Membrane (HET-CAM)

2.6.1. Preparation of Test Samples

KT-loaded NP (equivalent 100 µg KT.pellet^{-1}) and pure KT (100 µg.pellet^{-1}), SDS (50 mg SDS. pellet^{-1}) were suspended and dissolved in a 2.5% (w/v) agarose solution. For ease of application, the pellets of these solutions (10 mL) were prepared and applied dropwise on circular stainless-steel supports of 5 mm diameter and cooled to room temperature for solidification, and applied onto the chick chorioallantoic membrane (CAM).

2.6.2. In vivo HET-CAM Assay

The method was performed as described in the previous work. The previously incubated fertilized hen’s eggs for 72 h at 36.5°C and relative humidity of 80% were positioned in a horizontal position and rotated several times. The eggs were opened on the snub side, and furthermore, 10-15 mL of albumin was aspirated from them. The eggs were traced with a scalpel at two-third of the height (from the pointed side), and after that, the shells were removed with forceps. The cavity was covered with film, and they were incubated at 36.5°C at a relative humidity of 80% for a further 72h. Pellets (1 pellet.egg^{-1}) were placed on the CAM, which had approximately a diameter of 2 cm. One further day later the eggs were evaluated under the stereomicroscope. A total of 10-15 eggs were utilized for each test compound and the experiment was repeated three times for each test compound. Anti-inflammatory effects were evaluated by using a scoring system (Table **5**) and followed the conversion of the score index in the proportional inhibition of inflammation (Table **6**).

2.7. Statistical Analysis

Graphics were drawn with GraphPad Prism 7.0 software (GraphPad Software Inc., USA) and statistically analysed with one-way analysis of variance (ANOVA) and Tukey’s post hoc test. Results are expressed as mean ± standard deviation and the means of at least 2 independent experiments (n=8 for WST-1; n=3 for RT-PCR analysis), *n.s; $p>0.05$, *$p<0.05$, **$p<0.01$, ***$p<0.001$* and *****$p<0.0001$* were significant compared to the control group. Statistical analysis

Table 6. The score index in the proportional inhibition of inflammation.

Inhibition (%)	Anti-inflammatory Effect
≤ 40	No anti-inflammatory effect
40-55	Uncertain anti-inflammatory effect
55-70	Weak anti-inflammatory effect
70-85	Good anti-inflammatory effect
> 85	Strong anti-inflammatory effect

was performed using One-way ANOVA followed by Tukey's Multiple Comparison Test GraphPad Prism 6.0 statistical software for Windows for HET-CAM. Results were expressed as Mean ± standard deviation (Mean ± SD).

3. RESULTS AND DISCUSSION

Nanoformulation studies with KT are of great interest. In a study, chitosan-based NP systems were shown to be a promising candidate for the ocular application of KT in terms of increasing its efficacy and safety [34]. Dermal and transdermal administration of ketorolac is said to be an attractive alternative to avoid intramuscular injection and frequent dosing regimens, and in addition, ketorolac's high analgesic activity and low molecular weight make it a good candidate for transdermal administration [34, 35]. When the nanoformulations made with KT are examined, it is observed that our study is unique [35-40].

3.1. Characterization of Nanoparticles

PS, PDI, ZP and EE % values of NPs are shown in Table **7**. SEM images of pure KT and NPs are shown in Fig. (**1**). PSs are appropriate for topical application. All NPs presented PDI values lower than 0.5, and therefore particle size distribution was decided to be monodisperse [9]. Positive/Cationic ZP values of NPs highlighted the presence of the cationic ammonium group of ERS [17, 41, 42]. Fig. (**1**) clearly shows that the crystal structure of KT was diminished in the SEM image of KT-NP, indicating the successful loading of KT into the polymer. Fig. (**1**) indicated a mostly spherical smooth shape for all NPs [41]. When the literature on nanoparticle systems prepared with the nano spray dryer was examined, the particle sizes were observed in accordance with the literature. At the same time, when both particle size analyses and SEM images were compared in the relevant literature, aggregation and large particles were observed in the images, as in our study [17, 41, 43-49]. In conclusion, this situation is quite common in the literature and additional research is needed to establish a correlation between the two analyses.

In vitro dissolution profiles of pure KT and KT-NP coded formulation are shown in Fig. (**2**). The dissolution of KT from KT-NP continued over 24 hours, while pure KT exhibited a rapid release of 94.6% ± 3.3 (Mean ± SD) in 3 hours. The release rates observed from KT-NP coded formulations after 24 hours were 78.4% ± 2.9, demonstrating extended release from all formulations relative to pure KT [1, 50].

3.2. Effects of Ketorolac Tromethamine Loaded Nanoparticles on Fibroblast Cell Viability

According to the WST-1 results, 25, 50, 100, 200 and 400 μg.mL^{-1} KT concentrations increased the cell viability of BJ cells at a rate of 0.49, 0.27, 21.7, 24.61 and 38.24% in 24 hours, respectively, compared to the control group (Fig. **3**). The increase in cell viability was found significant at 200 (*p <0.05) and 400 (***p <0.001 μg/ml) KT concentrations.

According to the WST-1 results, 25, 50, 100, 200 and 400 μg.mL^{-1} KT-B (Blank) concentrations decreased the cell viability of BJ cells at a rate of 20.8, 28.02, 28.36, 28.11 and 44.83% in 24 hours, respectively, compared to the control group (Fig. **4**). All concentration groups significantly decreased the cell viability in a concentration-dependent manner.

Table 7. PS, PDI, ZP and EE % results.

Code	PS	PDI	ZP	EE%
KT-Blank (KT-B / KT-B-NP)	376.1 ± 7.3	0.36 ± 0.01	+41.7 ± 1.3	-
KT-NP	401.8 ± 9.4	0.37 ± 0.12	+40.6 ± 2.4	%72.8 ± 3.2

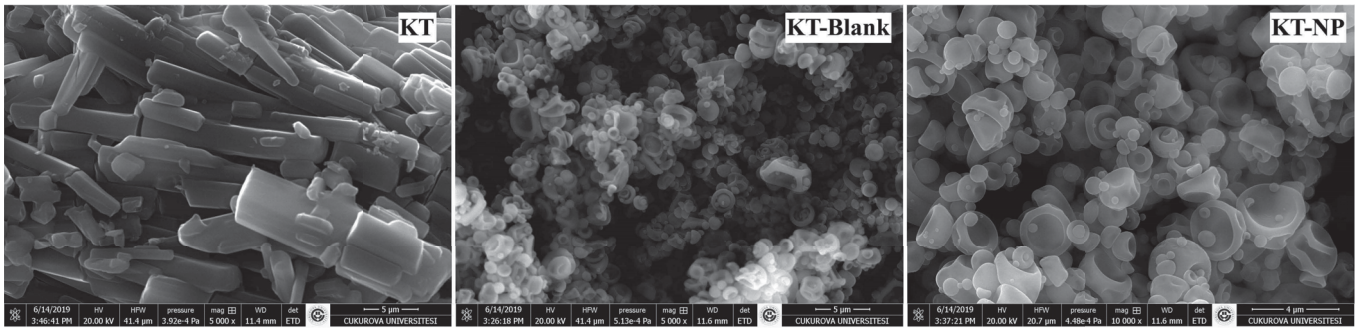

Fig. (1). SEM images of KT and NPs.

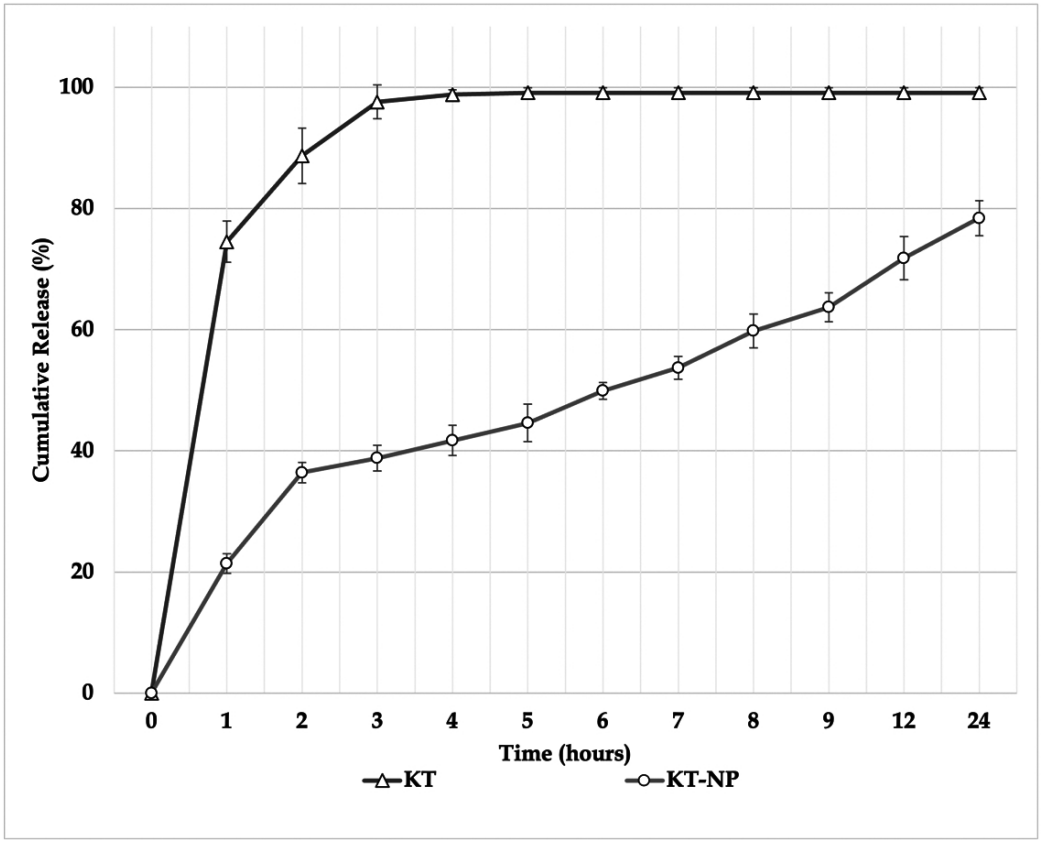

Fig. (2). *In vitro* dissolution profile of KT and KT-NP.

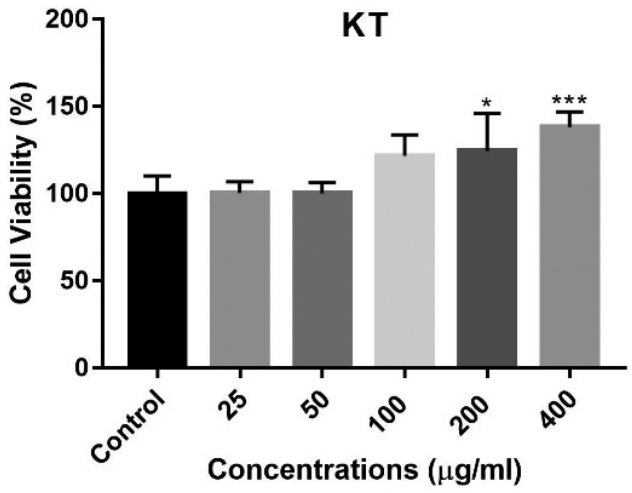

Fig. (3). Effects of KT on BJ cell viability. The error bars represent the standard deviations ((n = 8), p>0.05 not significant, *p <0.05, ***p <0.001 compared to the control group).

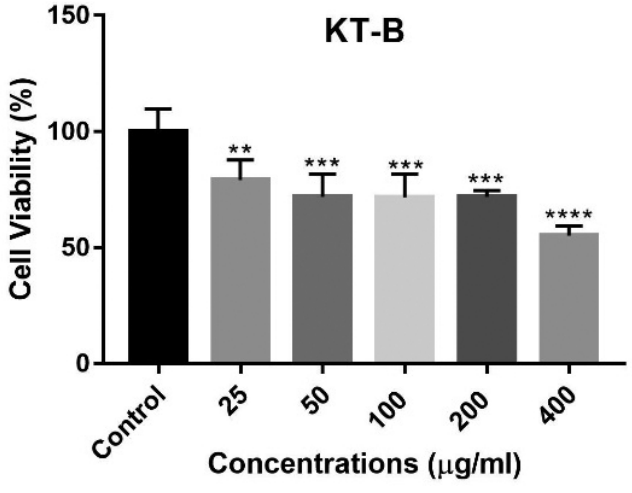

Fig. (4). Effects of KT-Blank (KT-B) on BJ cell viability. The error bars represent the standard deviations ((n = 8), **p <0.01, ***p <0.001 and ****p <0.0001 compared to the control group).

According to the WST-1 results, 25, 50, 100, 200 and 400 μg.mL^{-1} KT-NP concentrations increased the cell viability of BJ cells at a rate of 62.06, 52.09, 40.82, 16.07 and 12.46% in 24 hours, respectively, compared to the control group (Fig. **5**). The increase in cell viability was found significant at 25, 50 and 100 (****p <0.0001) μg/ml KT-NP concentrations.

Wound healing is distinguished by various stages, including the generation of new vessels, proliferation and differentiation of fibroblasts, deposition of the extracellular matrix (ECM) and re-epithelialization. Fibroblasts play a key role in this process, as wound closure involves fibroblast proliferation and migration to granulation tissue, followed by concurrent deposition of complex ECM elements, wound contraction, and

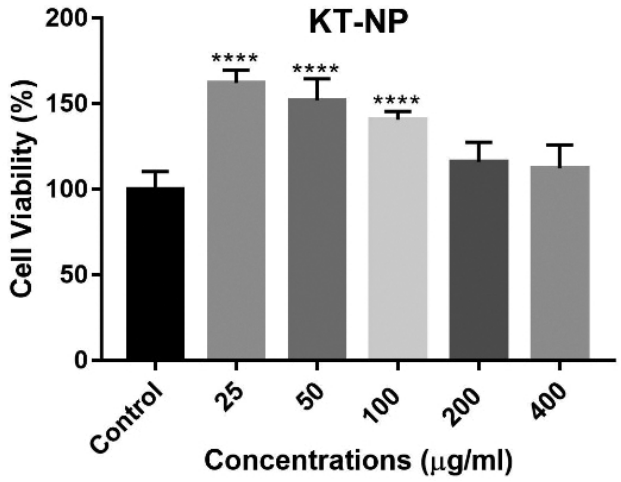

Fig. (5). Effects of KT-NP on BJ cell viability. The error bars represent the standard deviations ((n = 8), $p>0.05$ not significant, ****p <0.0001 compared to the control group).

remodeling. In particular, fibroblasts promote neoangiogenesis, secrete all ECM components (glycosaminoglycans, proteoglycans, glycoproteins and collagens) and generate many cytokines and growth factors [51]. Therefore, a cell viability assay was conducted to determine the effects of KT, KT-Blank [KT-B) and KT-NP on fibroblast cell proliferation associated with the wound healing process. According to the results, even though the solvent system (KT-Blank) reduced cell proliferation significantly, the lowest concentration of KT-NP increased the fibroblast cell proliferation higher than the highest concentration of KT because of the positive zeta potential of nanoparticles. Similar findings were obtained in a previous report, which investigated the effects of four topical analgesics, including KT, on human primary fibroblasts and keratinocytes. Based on the findings of this report, fibroblast proliferation was only significantly decreased at 10 mM KT concentration and increased with lower concentrations [52].

Only medications with the ideal balance of molecular weight, lipophilicity, and charge have been used in transdermal drug delivery systems. This situation imposes limitations on transdermal drug delivery systems [53]. Since the skin carries a negative surface charge as a result of phosphatidyl choline and carbohydrates found in human cells, which include negatively charged groups, cationic substances can also have a favorable impact on skin permeation [54-56]. In a study, it was determined that nanoemulsions with positive zeta potential values containing phytosphingosine, fludrocortisone acetate and flumethasone pivalate were more effective in skin diffusion from pig skin than negatively charged ones [56]. Likewise, in another study, it was stated that a positive charge is important for intracellular uptake [57]. In another study, it was determined that positively charged systems penetrate not only into the skin but also into the nucleus. The positive charge of the carbon point increases its affinity with anionic nucleic acids, making it easier to enter the nucleus [58]. As it is understood from the literature, the intracellular uptake and penetration of positively charged systems into the skin are quite good compared to negatively charged systems, and our study supports this issue.

3.3. Effects of Ketorolac Tromethamine Loaded Nanoparticles on COL1A1 Gene Expression Levels

Fibroblasts are ubiquitous mesenchymal cells that synthesize collagen and other matrix macromolecules for the structural protection of connective tissues. Collagen I is one of the dermal ECM proteins, which is primarily excreted by transforming growth factor-β (TGF-β)-activated dermal fibroblasts, a multifunctional growth factor that regulates the expression, deposition and turnover of extracellular matrix proteins in the skin [59]. The fibril-forming collagen type I, which is encoded by the COL1A1 gene, is the most common collagen in the skin, accounting for 90% of the total [60]. It is very important for wound healing as it is vital for the systemic organization, integrity, and strength of the tissue. Therefore, the effects on COL1A1 gene expression levels related with wound healing have been tested at the most effective concentrations of KT (400 $\mu g.mL^{-1}$) and KT-NP (25 $\mu g.mL^{-1}$) on fibroblast proliferation and COL1A1 expression levels were increased 5.94 and 25.08-fold, respectively (Fig. **6**). Target/reference Cp values of the results are shown in Table **8**.

The effects of KT on the healing of different wounds, including surgical [61], bone [62], fracture [63], anastomotic [64] and incisional [65], were investigated previously. In some of these studies, the effects of KT on collagen levels in different tissues were also investigated. However, the results differ according to the tissues. Similar results were obtained with a study in which analgesic effects of a ketorolac-eluting thermosensitive biodegradable hydrogel in the plantar incisional pain model of the rat hind-paw. According to the histologic analysis results, greater epithelialization and collagen deposition around the keto-hydrogel treated wounds linked with the better anti-inflammatory properties of the formulation were revealed [65]. Similarly, the 5-fold increased effect of KT-NP formulation on collagen gene expression compared to KT, is also related to the enhanced anti-inflammatory effect in line with the *in vivo* HET-CAM assay results.

3.4. *In vivo* HET-CAM Assay Result

We aimed to provide a high anti-inflammatory effect with a low dose to be determined by *in vivo* HET-CAM analysis as a new, popular, and *in vivo* animal experiment alternative method. Fig. (**7**) shows the anti-inflammatory effects of KT and KT-loaded NP.

The *in vivo* anti-inflammatory activity results indicated that the nanoparticle formulation, including ketorolac tromethamine as 100 $\mu g.pellet^{-1}$, showed significantly strong anti-inflammatory potential with 85.625 ± 11.825% inhibition value and no embryotoxicity, whereas ketorolac tromethamine showed weak activity with 60 ± 13.675% inhibition on the CAM. The anti-inflammatory activity of KT loaded NP formulations was examined using the *in vivo* HET-CAM assay. For the assay, SDS was used to cause irritation and hemorrhage on the CAM. The anti-inflammatory results are in Fig. (**2**). For the evaluation of the anti-

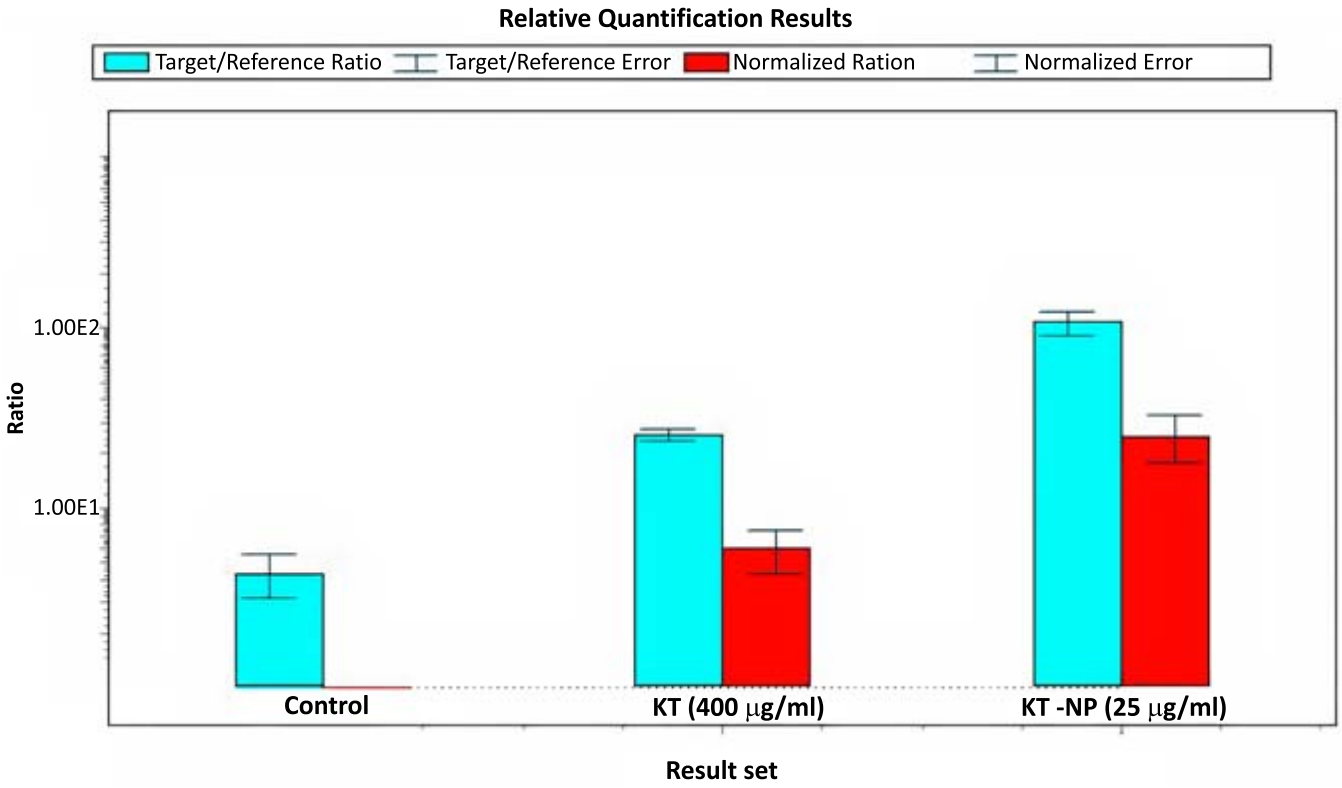

Fig. (6). Effects of KT and KT-NP on mRNA expression levels of COL1A1 gene (Bar-chart displays target/reference ratios, with normalized values in red). (*A higher resolution / colour version of this figure is available in the electronic copy of the article*).

Table 8. Target/reference values of COL1A1 mRNA expressions.

Sample Name	Target Name		Tgt Cp	Ref. Cp	Ratios		Corr/Multi Factor
	Targets	References	Mean	Mean	Tgt/Ref.	Nom	
Control	COL1A1	G6PD	32.14	34.24	4.290	1.000	1/1
KT-NP 25 ug/mL	COL1A1	G6PD	19.75	26.50	107.6	25.08	1/1
KT 400 ug/mL	COL1A1	G6PD	23.17	27.84	25.49	5.942	1/1

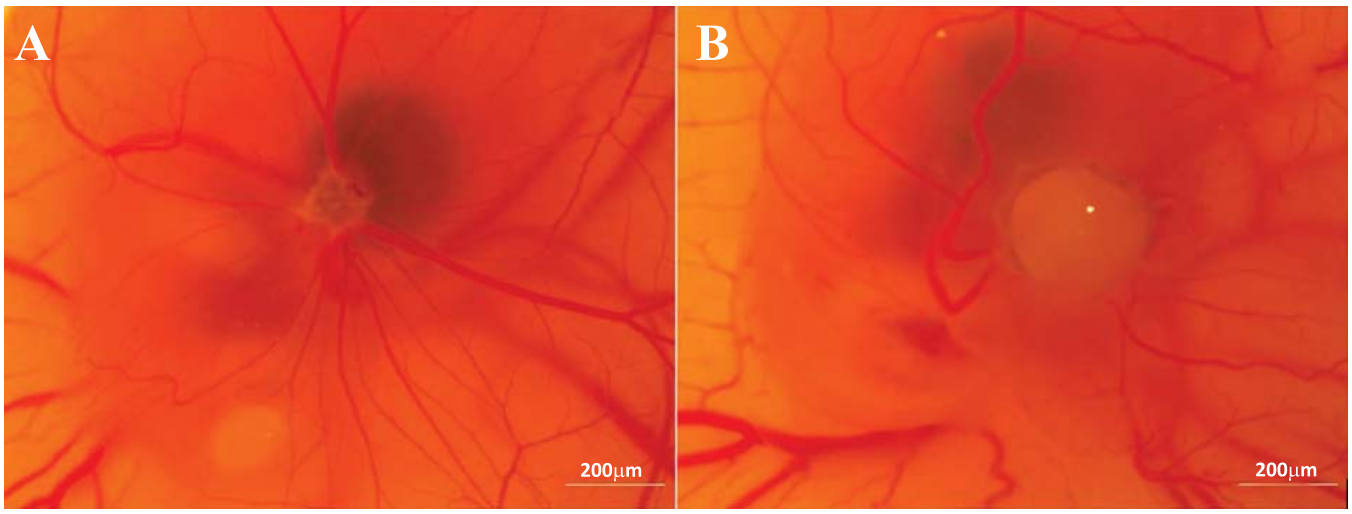

Fig. (7). The *in vivo* anti-inflammatory effects of KT and KT-loaded NP on the CAM. ((**A**): Weak anti-inflammatory effect of KT at 100 µg/pellet, (**B**): Strong anti-inflammatory activity of KT-NP including KT as 100 µg/pellet on the CAM). (*A higher resolution / colour version of this figure is available in the electronic copy of the article*).

inflammatory effect, a semi- quantitative score system is used, as shown in Table **5**, and a score index is described in Table **6**. In line with the HET-CAM results, it is thought that the anti-inflammatory activity has been increased with the nanoparticle structure, and thus a successful treatment can be obtained in the wound healing process. Similar results are found in the literature [23-25].

CONCLUSION

KT-loaded nanoparticles were produced in a nano-spray-drying device. All NPs presented PDI values lower than 0.5, and therefore particle size distribution was decided to be monodisperse. Positive/Cationic zeta potential values of NPs highlighted the presence of the cationic ammonium group of ERS. The release of KT from NP-1 continued over 24 hours, while pure KT exhibited a rapid release of 94.6% ± 3.3 (Mean ± SD) in 3 hours. The release rates observed from KT-NP coded formulations after 24 hours were 78.4% ± 2.9, demonstrating extended release from all formulations relative to pure KT. The lowest concentration of KT-NP increased fibroblast cell proliferation higher than the highest concentration of KT. The 5-fold increased effect of KT-NP formulation on collagen gene expression compared to KT is also related to the enhanced anti-inflammatory effect in line with the *in vivo* HET-CAM assay results. With the findings of the cell viability and gene expression tests, an effective nano-topical formulation, particularly for wound healing, is possible. With the HET-CAM results achieved, there is potential for a successful nano-topical formulation, both wound healing and antiinflamatuvar treatment.

LIST OF ABBREVIATIONS

COX	=	Cyclooxygenase
EE %	=	Encapsulation Efficiency %
ERS 100	=	Eudragit RS 100
HET- CAM	=	Hen's Egg Test on the Chorioallantoic Membrane
KT	=	Ketorolac Tromethamine
KT-Blank	=	Blank Formulation
KT-NP	=	Ketorolac Tromethamine Loaded Nanoparticle Formulation
NP	=	Nanoparticle
PDI	=	Polydispersity Index
PS	=	Particle Size
RT-PCR	=	Real-Time Polymerase Chain Reaction
SEM	=	Scanning Electron Microscope
$t_{1/2}$	=	Plasma Half-Life
UPLC	=	Ultra Performance Liquid Chromatography
ZP	=	Zeta potential

ETHICS APPROVAL AND CONSENT TO PARTICIPATE

Not applicable.

HUMAN AND ANIMAL RIGHTS

No animals/humans were used for studies that are basis of this research.

CONSENT FOR PUBLICATION

Not applicable.

AVAILABILITY OF DATA AND MATERIALS

Not applicable.

FUNDING

This study was financed by Anadolu University Scientific Research Project Foundation (Grant no: 2105S053).

CONFLICT OF INTEREST

The authors declare no conflict of interest, financial or otherwise.

ACKNOWLEDGEMENTS

Declared none.

REFERENCES

[1] Ozturk, A Design of cefaclor monohydrate containing nanoparticles with extended antibacterial effect by nano-spray dryer: A nanoenglobing study. *J. Res. Pharm,* **2020**, *24*(1), 100-111.

[2] Öztürk, K.; Eroğlu, H.; Çalış, S. Novel advances in targeted drug delivery. *J. Drug Target.,* **2018**, *26*(8), 633-642. http://dx.doi.org/10.1080/1061186X.2017.1401076 PMID: 29096554

[3] Öztürk, A.A.; Aygül, A.; Şenel, B. Influence of glyceryl behenate, tripalmitin and stearic acid on the properties of clarithromycin incorporated solid lipid nanoparticles (SLNs): Formulation, characterization, antibacterial activity and cytotoxicity. *J. Drug Deliv. Sci. Technol.,* **2019**, *54*, 101240. http://dx.doi.org/10.1016/j.jddst.2019.101240

[4] Öztürk, A.A.; Yenilmez, E.; Özarda, M.G. Clarithromycin-loaded poly (lactic-co-glycolic acid)(PLGA) nanoparticles for oral administration: Effect of polymer molecular weight and surface modification with chitosan on formulation, nanoparticle characterization and antibacterial effects. *Polymers,* **2019**, *11*(10), 1632. http://dx.doi.org/10.3390/polym11101632 PMID: 31600969

[5] Naz, M.Y.; Fatima, H.; Shukrullah, S.; Aslam, H.; Ullah, S.; Assiri, M.A. A review of multifunction smart nanoparticle based drug delivery systems. *Curr. Pharm. Des.,* **2022**, *28*(36), 2965-2983. http://dx.doi.org/10.2174/1381612828666220422085702 PMID: 35466867

[6] Fadilah, N.I.M.; Isa, I.L.M.; Zaman, W.S.W.K.; Tabata, Y.; Fauzi, M.B. The effect of nanoparticle-incorporated natural-based biomaterials towards cells on activated pathways: A systematic review. *Polymers,* **2022**, *14*(3), 476. http://dx.doi.org/10.3390/polym14030476 PMID: 35160466

[7] Alamdari, S.G.; Amini, M.; Jalilzadeh, N.; Baradaran, B.; Mohammadzadeh, R.; Mokhtarzadeh, A.; Oroojalian, F. Recent advances in nanoparticle-based photothermal therapy for breast cancer. *J. Control. Release,* **2022**, *349*, 269-303. http://dx.doi.org/10.1016/j.jconrel.2022.06.050 PMID: 35787915

[8] Afshari, A.R.; Sanati, M.; Mollazadeh, H.; Kesharwani, P.; Johnston, T.P.; Sahebkar, A. Nanoparticle-based drug delivery systems in cancer: A focus on inflammatory pathways. In: *Seminars in Cancer Biology.,* **2022**.

[9] Ekinci, M.; Öztürk, A.A.; Santos-Oliveira, R.; İlem-Özdemir, D. The use of Lamivudine-loaded PLGA nanoparticles in the diagnosis of lung cancer: Preparation, characterization, radiolabeling with 99mTc and cell binding. *J. Drug Deliv. Sci. Technol.,* **2022**, *69*, 103139. http://dx.doi.org/10.1016/j.jddst.2022.103139

[10] Chakraborty, A.; Haque, S.M.; Dey, D.; Mukherjee, S.; Ghosh, B. Phytogenic silver nanoparticles from tissue-cultured Kaempferia angustifolia — an underutilized medicinal herb: A comparative antibac-

terial study on urinary pathogens. *J. Genet. Eng. Biotechnol.,* **2022**, *20*(1), 131.
http://dx.doi.org/10.1186/s43141-022-00414-4 PMID: 36074190

[11] Babaie, S.; Taghvimi, A.; Hong, J.H.; Hamishehkar, H.; An, S.; Kim, K.H. Recent advances in pain management based on nanoparticle technologies. *J. Nanobiotechnology,* **2022**, *20*(1), 290.
http://dx.doi.org/10.1186/s12951-022-01473-y PMID: 35717383

[12] Abdelghany, T.M.; Al-Rajhi, A.M.; Almuhayawi, M.S.; Abada, E.; Al Abboud, M.A.; Moawad, H. Green fabrication of nanocomposite doped with selenium nanoparticle–based starch and glycogen with its therapeutic activity: Antimicrobial, antioxidant, and anti-inflammatory *in vitro*. *Biomass Convers. Biorefin.,* **2022**, 1-13.

[13] Jiang, W.; He, S.; Su, D.; Ye, M.; Zeng, Q.; Yuan, Y. Synthesis, characterization of tuna polypeptide selenium nanoparticle, and its immunomodulatory and antioxidant effects *in vivo*. *Food Chem.,* **2022**, *383*, 132405.
http://dx.doi.org/10.1016/j.foodchem.2022.132405 PMID: 35168050

[14] Yasamineh, S.; Kalajahi, H.G.; Yasamineh, P.; Yazdani, Y.; Gholizadeh, O.; Tabatabaie, R.; Afkhami, H.; Davodabadi, F.; farkhad, A.K.; Pahlevan, D.; Firouzi-Amandi, A.; Nejati-Koshki, K.; Dadashpour, M. An overview on nanoparticle-based strategies to fight viral infections with a focus on COVID-19. *J. Nanobiotechnology,* **2022**, *20*(1), 440.
http://dx.doi.org/10.1186/s12951-022-01625-0 PMID: 36209089

[15] Goyal, R.; Macri, L.K.; Kaplan, H.M.; Kohn, J. Nanoparticles and nanofibers for topical drug delivery. *J. Control. Release,* **2016**, *240*, 77-92.
http://dx.doi.org/10.1016/j.jconrel.2015.10.049 PMID: 26518723

[16] Öztürk, A.A.; Arpagaus, C. Nano spray-dried drugs for oral administration: A review. *Assay Drug Dev. Technol.,* **2021**, *19*(7), 412-441.
http://dx.doi.org/10.1089/adt.2021.053 PMID: 34550790

[17] Öztürk, A.A.; Yenilmez, E.; Arslan, R.; Şenel, B.; Yazan, Y. Dexketoprofen trometamol-loaded Kollidon® SR and Eudragit® RS 100 polymeric nanoparticles: Formulation and *in vitro - in vivo* evaluation. *Lat. Am. J. Pharm.,* **2017**, *36*(11), 2153-2165.

[18] Sinha, V.R.; Kumar, R.V.; Singh, G. Ketorolac tromethamine formulations: An overview. *Expert Opin. Drug Deliv.,* **2009**, *6*(9), 961-975.
http://dx.doi.org/10.1517/17425240903116006 PMID: 19663721

[19] Bryant, A.E.; Aldape, M.J.; Bayer, C.R.; Katahira, E.J.; Bond, L.; Nicora, C.D.; Fillmore, T.L.; Clauss, T.R.W.; Metz, T.O.; Webb-Robertson, B.J.; Stevens, D.L. Effects of delayed NSAID administration after experimental eccentric contraction injury – A cellular and proteomics study. *PLoS One,* **2017**, *12*(2), e0172486.
http://dx.doi.org/10.1371/journal.pone.0172486 PMID: 28245256

[20] Hadagali, M.D.; Chua, L.S. The anti-inflammatory and wound healing properties of honey. *Eur. Food Res. Technol.,* **2014**, *239*(6), 1003-1014.
http://dx.doi.org/10.1007/s00217-014-2297-6

[21] Hamdan, S.; Pastar, I.; Drakulich, S.; Dikici, E.; Tomic-Canic, M.; Deo, S.; Daunert, S. Nanotechnology-driven therapeutic interventions in wound healing: Potential uses and applications. *ACS Cent. Sci.,* **2017**, *3*(3), 163-175.
http://dx.doi.org/10.1021/acscentsci.6b00371 PMID: 28386594

[22] Zhang, J.M.; An, J. Cytokines, inflammation, and pain. *Int. Anesthesiol. Clin.,* **2007**, *45*(2), 27-37.
http://dx.doi.org/10.1097/AIA.0b013e318034194e PMID: 17426506

[23] Öztürk, A.A.; Yenilmez, E.; Şenel, B.; Kıyan, H.T.; Güven, U.M. Effect of different molecular weight PLGA on flurbiprofen nanoparticles: Formulation, characterization, cytotoxicity, and *in vivo* anti-inflammatory effect by using HET-CAM assay. *Drug Dev. Ind. Pharm.,* **2020**, *46*(4), 682-695.
http://dx.doi.org/10.1080/03639045.2020.1755304 PMID: 32281428

[24] Öztürk, A.A.; Namlı, İ.; Güleç, K.; Kıyan, H.T. Diclofenac sodium loaded PLGA nanoparticles for inflammatory diseases with high anti-inflammatory properties at low dose: Formulation, characterization and *in vivo* HET-CAM analysis. *Microvasc. Res.,* **2020**, *130*, 103991.
http://dx.doi.org/10.1016/j.mvr.2020.103991 PMID: 32105668

[25] Öztürk, A.A.; Kıyan, H.T. Treatment of oxidative stress-induced pain and inflammation with dexketoprofen trometamol loaded different molecular weight chitosan nanoparticles: Formulation, characterization and anti-inflammatory activity by using *in vivo* HET-CAM assay. *Microvasc. Res.,* **2020**, *128*, 103961.
http://dx.doi.org/10.1016/j.mvr.2019.103961 PMID: 31758946

[26] Öztürk, A.A.; Gündüz, A.B.; Ozisik, O. Supervised machine learning algorithms for evaluation of solid lipid nanoparticles and particle size. *Comb. Chem. High Throughput Screen.,* **2019**, *21*(9), 693-699.
http://dx.doi.org/10.2174/1386207322666181218160704 PMID: 30569864

[27] Yurtdas, K.G; Ozturk, A. Levocetirizine dihydrochloride-loaded chitosan nanoparticles: Formulation and *in vitro* evaluation. *Turk. J. Pharm. Sci.,* **2020**, *17*(1), 27-35.
http://dx.doi.org/10.4274/tjps.galenos.2018.34392 PMID: 32454757

[28] Öztürk, A.A.; Namlı, İ.; Güleç, K.; Görgülü, Ş. Design of lamivudine loaded nanoparticles for oral application by nano spray drying method: A new approach to use an antiretroviral drug for lung cancer treatment. *Comb. Chem. High Throughput Screen.,* **2020**, *23*(10), 1064-1079.
http://dx.doi.org/10.2174/1386207323666200325155020 PMID: 32209039

[29] Öztürk, A.A.; Güven, U.M. Cefaclor monohydrate loaded microemulsion formulation for topical application: Characterization with new developed UPLC method and stability study. *J. Res. Pharm.,* **2019**, *23*(3), 426-440.
http://dx.doi.org/10.12991/jrp.2019.150

[30] Öztürk, AA; Güven, UM; Yenilmez, E Flurbiprofen loaded gel based topical delivery system: Formulation and *in vitro* characterization with new developed UPLC method. *ACTA Pharmaceutica Sciencia,* **2018**, *56*(4), 81-105.

[31] Dikmen, M.; Öztürk, S.E.; Cantürk, Z.; Ceylan, G.; Karaduman, A.B.; Yamaç, M. Anticancer and antimetastatic activity of Hypomyces chrysospermus, a cosmopolitan parasite in different human cancer cells. *Mol. Biol. Rep.,* **2020**, *47*(5), 3765-3778.
http://dx.doi.org/10.1007/s11033-020-05468-6 PMID: 32378168

[32] Engür, S.; Dikmen, M. The evaluation of the anti-cancer activity of ixazomib on Caco2 colon solid tumor cells, comparison with bortezomib. *Acta Clin. Belg.,* **2017**, *72*(6), 391-398.
http://dx.doi.org/10.1080/17843286.2017.1302623 PMID: 28327055

[33] Dikmen, M.; Canturk, Z.; Tilki, E.K.; Engur, S. Evaluation of antiangiogenic and antimetastatic Effects of *Penicillium chrysogenum* Secondary Metabolites. *Indian J. Pharm. Sci.,* **2017**, *79*(1), 49-57.
http://dx.doi.org/10.4172/pharmaceutical-sciences.1000200

[34] Fathalla, Z.M.A.; Khaled, K.A.; Hussein, A.K.; Alany, R.G.; Vangala, A. Formulation and corneal permeation of ketorolac tromethamine-loaded chitosan nanoparticles. *Drug Dev. Ind. Pharm.,* **2016**, *42*(4), 514-524.
http://dx.doi.org/10.3109/03639045.2015.1081236 PMID: 26407208

[35] Archna, SSG; Mishra, MK; Prasad, RK Formulation and characterization of ketorolac tromethamine nanoparticle with eudragit RS-100 and RL-100 by nano precipitation method. *Int. J. Res.,* **2017**, *17*, 17-23.

[36] Goerne, L; López García, M; Rodríguez Grada, G; Ortiz Pérez, I; Gómez López, E; Lemus, A. Obtaining of sol-gel ketorolac-silica nanoparticles: Characterization and drug release kinetics. *J. Nanomaterials.,* **2013**, Article ID 450483.

[37] Mohammadi, G.; Mirzaeei, S.; Taghe, S.; Mohammadi, P. Preparation and evaluation of Eudragit® L100 nanoparticles loaded impregnated with KT tromethamine loaded PVA-HEC insertions for ophthalmic drug delivery. *Adv. Pharm. Bull.,* **2019**, *9*(4), 593-600.
http://dx.doi.org/10.15171/apb.2019.068 PMID: 31857963

[38] Morsi, N.; Ghorab, D.; Refai, H.; Teba, H. Preparation and evaluation of alginate/chitosan nanodispersions for ocular delivery. *Int. J. Pharm. Pharm. Sci.,* **2015**, *7*(7), 234-240.

[39] Jadhav, P.A.; Yadav, A.V. Design, development and characterization of ketorolac tromethamine polymeric nanosuspension. *Ther. Deliv.,* **2019**, *10*(9), 585-597.
http://dx.doi.org/10.4155/tde-2019-0045 PMID: 31581882

[40] Salvi, V.; Pawar, P. Eudragit RL100 based moxifloxacin hydrochloride and ketorolac tromethamine combination nanoparticulate system for ocular drug delivery. *Pharm. Nanotechnol.,* **2020**, *8*(2), 133-147.
http://dx.doi.org/10.2174/2211738508666200313140902 PMID: 32167436

[41] Öztürk, AA; Güven, UM; Yenilmez, E; Şenel, B Effects of different derivatives of eudragit polymer on entrapment efficiency, *in vitro* dissolution, release kinetics and cell viability results on extended release flurbiprofen loaded nanomedicines. *Lat. Am. J. Pharm,* **2018**, *37*(10), 1981.

[42] Guven, UM; Ozturk, AA; Yenilmez, E Evaluation of carvedilol-loaded Eudragit nanoparticles. *MARMARA Pharm. J,* **2020**, *24*(1), 71-81.
[43] Yenilmez, E. Desloratadine-Eudragit® RS100 nanoparticles: Formulation and characterization. *Turk. J. Pharm. Sci.,* **2017**, *14*(2), 148-156. http://dx.doi.org/10.4274/tjps.52523 PMID: 32454606
[44] El-Maghawry, E.; Tadros, M.I.; El-Kheshen, S.A.; Abd-Elbary, A. Eudragit®-S100 coated PLGA nanoparticles for colon targeting of Etoricoxib: optimization and pharmacokinetic assessments in healthy human volunteers. *Int. J. Nanomedicine,* **2020**, *15*, 3965-3980. http://dx.doi.org/10.2147/IJN.S244124 PMID: 32606658
[45] Yurtdaş-Kırımlıoğlu, G.; Güleç, K.; Görgülü, Ş.; Kıyan, H.T. Oseltamivir phosphate loaded pegylated-Eudragit nanoparticles for lung cancer therapy: Characterization, prolonged release, cytotoxicity profile, apoptosis pathways and *in vivo* anti-angiogenic effect by using CAM assay. *Microvasc. Res.,* **2022**, *139*, 104251. http://dx.doi.org/10.1016/j.mvr.2021.104251 PMID: 34520775
[46] Oliveira, A.M.; Guimarães, K.L.; Cerize, N.N.P.; Tunussi, A.S.; Poço, J.G.R. Nano spray drying as an innovative technology for encapsulating hydrophilic active pharmaceutical ingredients (API). *J. Nanomed. Nanotechnol.,* **2013**, *4*(6) http://dx.doi.org/10.4172/2157-7439.1000186
[47] Muchtaridi, M.; Herdiana, Y.; Handaresta, D.F.; Joni, I.M.; Wathoni, N. Synthesis of nano-α mangostin based on chitosan and Eudragit S 100. *J. Adv. Pharm. Technol. Res.,* **2020**, *11*(3), 95-100. http://dx.doi.org/10.4103/japtr.JAPTR_182_19 PMID: 33102191
[48] Abdel-Mageed, H.M.; Fouad, S.A.; Teaima, M.H.; Abdel-Aty, A.M.; Fahmy, A.S.; Shaker, D.S.; Mohamed, S.A. Optimization of nano spray drying parameters for production of α-amylase nanopowder for biotheraputic applications using factorial design. *Dry. Technol.,* **2019**, *37*(16), 2152-2160. http://dx.doi.org/10.1080/07373937.2019.1565576
[49] Öztürk, AA; Yenilmez, E; Yazan, Y Dexketoprofen trometamol-loaded Eudragit® RL 100 nanoparticle formulation, characterization and release kinetics. *Acta Pharmaceut. Sci.,* **2019**, *57*(1), 69-84.
[50] Alper Öztürk, A.; Namlı, İ.; Aygül, A. Cefaclor monohydrate-loaded colon-targeted nanoparticles for use in COVID-19 dependent coinfections and intestinal symptoms: Formulation, characterization, release kinetics, and antimicrobial activity. *Assay Drug Dev. Technol.,* **2021**, *19*(3), 156-175. http://dx.doi.org/10.1089/adt.2020.1014 PMID: 33728979
[51] Stortelers, C.; Kerkhoven, R.; Moolenaar, W.H. Multiple actions of lysophosphatidic acid on fibroblasts revealed by transcriptional profiling. *BMC Genomics,* **2008**, *9*(1), 387. http://dx.doi.org/10.1186/1471-2164-9-387 PMID: 18702810
[52] Harris, K.L.; Bainbridge, N.J.; Jordan, N.R.; Sharpe, J.R. The effect of topical analgesics on *ex vivo* skin growth and human keratinocyte and fibroblast behavior. *Wound Repair Regen.,* **2009**, *17*(3), 340-346. http://dx.doi.org/10.1111/j.1524-475X.2009.00488.x PMID: 19660041
[53] Honary, S.; Zahir, F. Effect of zeta potential on the properties of nano-drug delivery systems-a review (Part 1). *Trop. J. Pharm. Res.,* **2013**, *12*(2), 255-264.
[54] Chang, J.H.; Cho, M.A.; Son, H.H.; Lee, C.K.; Yoon, M.S.; Cho, H.H. Characterization and formation of phospholipid nanoemulsion coatings on Mg-modified sericite surface. *J. Ind. Eng. Chem.,* **2006**, *12*(4), 635-638.
[55] Campbell, R.B. Positively-charged liposomes for targeting tumor vasculature. In: *Nanotechnology for cancer therapy*; CRC Press, Boca Raton, **2006**; pp. 613-627.
[56] Hoeller, S.; Sperger, A.; Valenta, C. Lecithin based nanoemulsions: A comparative study of the influence of non-ionic surfactants and the cationic phytosphingosine on physicochemical behaviour and skin permeation. *Int. J. Pharm.,* **2009**, *370*(1-2), 181-186. http://dx.doi.org/10.1016/j.ijpharm.2008.11.014 PMID: 19073240
[57] Şenel, B.; Öztürk, A.A. New approaches to tumor therapy with siRNA-decorated and chitosan-modified PLGA nanoparticles. *Drug Dev. Ind. Pharm.,* **2019**, *45*(11), 1835-1848. http://dx.doi.org/10.1080/03639045.2019.1665061 PMID: 31491363
[58] Han, G.; Zhao, J.; Zhang, R.; Tian, X.; Liu, Z.; Wang, A.; Liu, R.; Liu, B.; Han, M.Y.; Gao, X.; Zhang, Z. Membrane-penetrating carbon quantum dots for imaging nucleic acid structures in live organisms. *Angew. Chem. Int. Ed.,* **2019**, *58*(21), 7087-7091. http://dx.doi.org/10.1002/anie.201903005 PMID: 30912239
[59] Krieg, T.; Aumailley, M. The extracellular matrix of the dermis: Flexible structures with dynamic functions. *Exp. Dermatol.,* **2011**, *20*(8), 689-695. http://dx.doi.org/10.1111/j.1600-0625.2011.01313.x PMID: 21615511
[60] Gelse, K.; Pöschl, E.; Aigner, T. Collagens-Structure, function, and biosynthesis. *Adv. Drug Deliv. Rev.,* **2003**, *55*(12), 1531-1546. http://dx.doi.org/10.1016/j.addr.2003.08.002 PMID: 14623400
[61] Haws, M.J.; Kucan, J.O.; Roth, A.C.; Suchy, H.; Brown, R.E. The effects of chronic ketorolac tromethamine (toradol) on wound healing. *Ann. Plast. Surg.,* **1996**, *37*(2), 147-151. http://dx.doi.org/10.1097/00000637-199608000-00005 PMID: 8863973
[62] Reikeraas, O.; Engebretsen, L. Effects of ketoralac tromethamine and indomethacin on primary and secondary bone healing. *Arch. Orthop. Trauma Surg.,* **1998**, *118*(1-2), 50-52. http://dx.doi.org/10.1007/s004020050310 PMID: 9833106
[63] Mullis, B.H.; Copland, S.T.; Weinhold, P.S.; Miclau, T.; Lester, G.E.; Bos, G.D. Effect of COX-2 inhibitors and non-steroidal anti-inflammatory drugs on a mouse fracture model. *Injury,* **2006**, *37*(9), 827-837. http://dx.doi.org/10.1016/j.injury.2005.12.018 PMID: 16497308
[64] Ghiselli, R.; Lucarini, G.; Ortenzi, M.; Salvolini, E.; Saccomanno, S.; Orlando, F.; Provinciali, M.; Casciani, F.; Guerrieri, M. Anastomotic healing in a rat model of peritonitis after non-steroidal anti-inflammatory drug administration. *Eur. J. Histochem.,* **2020**, *64*(1), 3085. http://dx.doi.org/10.4081/ejh.2020.3085 PMID: 31941266
[65] Wu, M.H.; Shih, M.H.; Hsu, W.B.; Dubey, N.K.; Lee, W.F.; Lin, T.Y.; Hsieh, M.Y.; Chen, C.F.; Peng, K.T.; Huang, T.J.; Shi, C.S.; Guo, R.S.; Cai, C.J.; Chung, C.Y.; Wong, C.H. Evaluation of a novel biodegradable thermosensitive keto-hydrogel for improving postoperative pain in a rat model. *PLoS One,* **2017**, *12*(10), e0186784. http://dx.doi.org/10.1371/journal.pone.0186784 PMID: 29059223

NEW The power of the Web of Science™ on your mobile device, wherever inspiration strikes. Dismiss Learn More

Already have a manuscript?

Use our Manuscript Matcher to find the best relevant journals!

Find a Match

Filters Clea

Web of Science Coverage

Open Access

Category

Country / Region

Language

Frequency

Journal Citation Reports

Refine Your Search Results

Current Drug Delivery

Search

Sort By: Relevancy

Search Results

Found 11,431 results (Page 1)

Share These Results

Exact Match Found

CURRENT DRUG DELIVERY

Publisher:	BENTHAM SCIENCE PUBL LTD , EXECUTIVE STE Y-2, PO BOX 7917, SAIF ZONE, SHARJAH, U ARAB EMIRATES, 1200 BR
ISSN / eISSN:	1567-2018 / 1875-5704
Web of Science Core Collection:	Science Citation Index Expanded
Additional *Web of Science* Indexes:	Biological Abstracts | BIOSIS Previews | Essential Science Indicators

5